Published in final edited form as:
Environ Sci Technol. 2013 December 3; 47(23): 13813–13821. doi:10.1021/es403264d.

High resolution analytical electron microscopy reveals cell culture media induced changes to the chemistry of silver nanowires

Shu Chen[1], **Ioannis G. Theodorou**[1], **Angela E. Goode**[1], **Andrew Gow**[2], **Stephan Schwander**[3], **Junfeng (Jim) Zhang**[4], **Kian Fan Chung**[5], **Teresa D. Tetley**[5], **Milo S. Shaffer**[6], **Mary P. Ryan**[1,*], and **Alexandra E. Porter**[1,*]

[1]Department of Materials and London Centre for Nanotechnology, Imperial College London, Exhibition Road, London SW7 2AZ, UK

[2]Department of Pharmacology and Toxicology at Rutgers University, Piscataway, NJ, USA

[3]Department of Environmental and Occupational Health, University of Medicine and Dentistry (UMDNJ) School of Public Health, New Jersey, USA

[4]Department of Preventive Medicine, Keck School of Medicine, University of Southern California, USA

[5]National Heart and Lung Institute, Imperial College London, UK

[6]Department of Chemistry and London Centre for Nanotechnology, Imperial College London, Exhibition Road, London SW7 2AZ, UK

Abstract

There is a growing concern about the potential adverse effects on human health upon exposure to engineered silver nanomaterials (particles, wires and plates). However, the majority of studies testing the toxicity of silver nanomaterials have examined nominally ‘as-synthesized’ materials without considering the fate of the materials in biologically relevant fluids. Here, in-house silver nanowires (AgNWs) were prepared by a modified polyol process and were incubated in three cell culture media (DMEM, RPMI-1640 and DCCM-1) to examine the impact of AgNW-medium interactions on the physicochemical properties of the AgNWs. High-resolution analytical transmission electron microscopy revealed that Ag_2S crystals form on the surface of AgNWs within 1 hour of incubation in DCCM-1. In contrast, the incubation of AgNWs in RPMI-1640 or DMEM did *not* lead to sulfidation. When the DCCM-1 cell culture medium was separated into its small molecule solutes and salts and protein components, the AgNWs were found to sulfidize in the fraction containing small molecule solutes and salts, but not in the fraction containing the protein component of the media. Further investigation showed the AgNWs did not readily

[*](A.E.P.) Phone: (+44)2075949691; fax: (+44)2075945017; a.e.porter@imperial.ac.uk. [*](M.P.R.) Phone: (+44)2075946755; fax: (+44)2075945017; m.p.ryan@imperial.ac.uk.

ASSOCIATED CONTENT

Experimental protocols, crystal information of various silver compounds, formulation of cell cluture media, EM characterization of AgNWs after various incubation conditions. ICP-OES analysis of sulfur content, pH measurements of cell culture media incubated with AgNWs are presented in supporting information. This material is available free of charge via the Internet: http://pubs.acs.org.

The authors declare no competing financial interest

sulfidize in the presence of isolated sulfur containing amino acids or proteins, such as cysteine or bovine serum albumin (BSA). The results demonstrate that the AgNWs can be transformed by the media before and during the incubation with cells and therefore the effects of cell culture media must be considered in the analysis of toxicity assays. Appropriate media and material controls must be in place to allow accurate predictions about the toxicity, and ultimately, the health risk of this commercially relevant class of nanomaterial.

Keywords

Silver; nanowires; sulfidation; cell culture media; proteins

Introduction

Silver nanomaterials are widely used in consumer products, including electronic and photonic devices as well as textiles, food storage containers and antiseptic sprays. These applications are in part driven by the well-known antibacterial activity of silver,[1–4] but there is also an increasing use for optoelectronic applications. An increase in the number of products containing silver nanomaterials will lead to a larger release in the environment during manufacture, use, washing or disposal of the products. Therefore, there is a growing concern about the potential adverse effects on human health upon exposure to Ag nanomaterials. These concerns have put nanosilver into the focus of intensive investigation. Elemental silver was considered to be of low toxicity to humans, despite the fact that several cases had been reported of argyria (irreversible pigmentation of the skin) or argyrosis (irreversible pigmentation of the eyes) after chronic ingestion of colloidal silver.[5, 6] The toxicity of silver nanoparticles (AgNPs) has been demonstrated for several species of vertebrates, invertebrates, and prokaryotic and eukaryotic microorganisms, as well as some mammalian cell-lines[3, 7]. The toxicological outcomes upon exposure to Ag nanomaterials may include oxidative stress, lipid peroxidation, inhibition of mitochondrial activity, damage of DNA and cell apoptosis[8–17]. Although several physicochemical properties of the particles (e.g. shape[13], size[9] and surface coating[11]) seem to play a role in the bioreactivity of Ag nanomaterials, the exact mechanism underlying the reactivity of Ag nanostructures remains elusive.

Several studies have linked the toxicity of AgNPs to their dissolution and the release of free Ag^+ ions[17]. Ag^+ can react with enzymes of the respiratory chain reaction, resulting in a disruption of ATP production, or binding to transport proteins leading to proton leakage[18–20]. One argument is that these effects are driven by the high affinity of Ag^+ with thiol groups present in the cysteine residues of the relevant enzymes or proteins[19]. Ag^+ ions can also enter the intracellular environment and trigger the generation of reactive oxygen species (ROS) through redox reactions with oxygen, causing membrane and DNA damage[21]. Some studies have suggested that particle surface reactions, which generate ROS or catalyze the oxidation of cellular components, could be a possible mechanism of toxicity[22]. Others propose direct damage to the cell membrane, leading to increased permeability and disruption of respiration[23]. Although these particle-specific mechanisms are highly debatable, there is a wide consensus that Ag^+ ion release is a major pathway for

the biological activity of nanosilver. Nevertheless, published results concerning the dissolution of AgNPs and the extent to which it affects toxicity are conflicting, with studies suggesting that AgNP toxicity can be attributed solely to ionic release of Ag^+ [24, 25] or coupled ionic-particle effects.[26–29] A possible reason for the lack of consistency could be the fact that most studies have neglected possible reactions of Ag nanomaterials with other species in their environment, which could lead to their chemical transformation and an alteration of their properties before, or during, cell exposure tests.

Although silver is considered a noble metal, it is far from being chemically inert. Metallic silver is not thermodynamically stable under environmental conditions and has been shown to oxidize or react with various organic and inorganic ligands[30, 31]. For example, the atmospheric sulfidation of bulk silver upon exposure to different S-bearing gases (H_2S, SO_2, OCS and CS_2) has been studied extensively[32, 33]. Sulfidation of Ag surfaces leads to the formation of a Ag_2S adlayer, which is very stable due to its extremely low solubility ($K_{sp}=5.92\times10^{-51}$)[34]. However, the sulfidation of silver nanostructures and the potential impact of this process on their properties has only recently attracted attention. For example, it was reported the secondary silver sulfide or selenide NPs formation in the skin formed by partial dissolution ingested particle in the GI tract followed by ions uptake and systemic circulation.[35] We also recently reported the transformation of AgNWs to silver sulfidation in lung epithelial cells, which acts as a potential detoxification mechanism.[36] Therefore, the fact that most of the toxicity studies performed on AgNPs so far have overlooked their possible sulfidation, either inadvertently during storage or, more significantly, intrinsically during the experiments, might be one of the reasons to have led to inconsistent results. Consequently, further investigation is required to understand how different sources of sulfur in the cellular environment can affect the mechanism and kinetics of Ag^+ ion release and Ag sulfidation.

The purpose of this study is to provide insights into the effect of the cell culture media and small molecule solutes and salts and proteins present within these media on the chemistry of AgNWs. Any transformation of the AgNWs in the cell culture medium could change their reactivity and impact their effects on cell metabolism, ultimately altering the toxicological outcome. It is therefore of vital importance to improve this understanding, to distinguish between physiological effects or artifacts introduced by the cell culture system. Three different cell culture media were studied in this work: DMEM, RPMI-1640 and DCCM-1. DMEM and RPMI-1640 were chosen because they are popular media used for cell culture. DCCM-1 is a serum free medium which has been commonly used to culture human epithelial cells. In contrast to RPMI-1640 and DMEM, DCCM-1 contains proteins and may therefore provide clues about the role of proteins on the chemical transformation of AgNWs. X-ray diffraction (XRD) and inductively coupled plasma–optical emission spectroscopy (ICP-OES) are commonly used bulk analytical techniques to characterize the crystal structures present in the sample and metal dissolution rates in different media. However, both of these techniques have limitations. For example, XRD cannot provide spatially resolved information about the distribution of crystal phases or the crystallinity of very small nanomaterial. ICP-OES detects the total metal content without distinguishing between metal oxidation states, therefore the dissolved metal ions must be separated from NPs in the solution to study dissolution rate. In this work, ICP-OES is shown to be an unsuitable

technique for measuring the silver dissolution rates in cell culture media, as insoluble silver compounds are formed. Transformation of the surface chemistry of the AgNWs in cell culture media was characterized using a set of spatially resolved, analytical transmission electron microscopy (TEM) techniques. The combination of TEM techniques applied provide high spatial resolution of the chemistry and crystallinity of the AgNWs and revealed detailed information about mechanism by which the AgNWs transform in different cell culture media. This information is important to understand how the biological environment controls the bioreactivity of Ag nanomaterials.

Results and Discussion

The AgNWs used in this study were fabricated in-house, in order to ensure a good control over their morphology, dimensions and chemistry. The synthesis was based on the polyol process developed by Xia *et al*.,[37] and optimized to reduce the formation of AgNPs in the final product, as well as excluding impurities from the system. As PVP has a stronger interaction with AgNWs {100} facets than {111} facets, this passivation effect of PVP on {111} facts lead to the formation of AgNWs. In addition, the capping of PVP on the AgNWs surface (SI, Fig 1S) also provides the stabilization effect to prevent NWs aggregation.[38] The synthesis was successful (Fig. 1a) with a bimodal length distribution (Fig. 1b), with an average length of 2.8 ± 2.4 μm and 7.0 ± 2.0 μm, respectively. The mean diameter of the AgNWs (Fig. 1c) was 129 ± 74 nm. A small fraction of AgNPs (about 1vol %) with a mean diameter of 126 ± 60 nm were mixed with the AgNWs (SI, Fig. 2S). The morphology and crystallinity of the AgNWs were characterized using BF-TEM (Fig. 1d), phase contrast HRTEM (Fig. 1e) and SAED (Fig. 1f). The lattice spacing of the AgNWs was 0.235 ± 0.007 nm and 0.210 ± 0.006 nm, which corresponds to the interplanar spacing of bulk Ag (111) and (200) lattice planes, respectively (Ref. #01-087-0597). The interplanar spacings measured from the SAED patterns were 0.241 ± 0.007, 0.209 ± 0.006, 0.148 ± 0.005, 0.127 ± 0.004 and 0.121 ± 0.004 nm, which are consistent with the bcc form of bulk Ag (Ref. #01-087-0597). An EDX spectrum taken from the AgNWs (Fig. 1h) confirmed that they were composed of pure silver.

After incubating AgNWs in DCCM-1 for 1 h at physiological temperature, their morphology was altered with respect to that of the original AgNWs (Fig. 2a). Instead of having smooth facets, the formation of small crystals was observed on the surface of the AgNWs. The interplanar spacings obtained from the SAED pattern were 0.335 ± 0.10, 0.309 ± 0.09, 0.284 ± 0.09 and 0.250± 0.08 nm, and correspond to the (012), (111), (−112) and (022) interplanar spacings of monoclinic Ag_2S, respectively (Ref. #00-014-0072). Note that these interplanar spacings do not match with the crystal structure of other common Ag compounds (Ag_2O (Ref. #00-041-1104) or AgCl (Ref. #00-031-1238), SI Table 1S). By using TEM technique, electrons can penetrate through the shell and reach the core to reveal the core crystal information. By optimising the sample height or focus conditions, atomic planes of the same height in the core and the edge can be focused at the same time to reveal the core and shell crystal information simultaneously. Phase contrast HR-TEM (Fig. 2b) revealed that the lattice spacings of the crystals formed at the surface of the AgNWs are ~0.26 nm and 0.22 nm, corresponding to the (112) and (031) lattice spacings of Ag_2S, respectively. In contrast, the lattice spacings of the core of the nanowires (~0.23 nm and 0.20 nm) correspond to the

interplanar spacings of metallic Ag. The formation of Ag_2S on the surface of the wires was supported by EDX analysis (Fig. 2c-bottom, a STEM-EDX line scan collected across the NW is presented in SI, Fig 3S.) and since neither O nor Cl was detected, the formation of Ag_2O or AgCl can be ruled out. In fact, the sulfidation of AgNWs in DCCM-1 was very fast, as the formation of Ag_2S on their surface could already be observed within 0.25 h of incubation (SI, Fig. 4S). On the other hand, when AgNWs were incubated in DMEM and RPMI-1640, no changes in their morphology or chemistry were detected. Typical HAADF-STEM images and EDX spectra of the AgNWs are given in Fig. 2d–e and show that the AgNWs do not change their morphology, suggesting that they are stable in DMEM and RPMI-1640.

ICP-OES study and pH measurement were carried out to measure the silver dissolution rate. The amount of solubilized silver released was below the signal to noise ratio at all-time points, in DI-water and all cell culture media (Fig.3a). The low solubilized silver level detected in the cell media is expected because of formation of insoluble silver compounds. ICP-OES is a sensitive analytical technique, and is therefore widely used for dissolution studies of metal based NPs.[39, 40] In order to distinguish dissolved metal ions from the NPs, a separation process, often achieved by centrifugation, ultrafiltration or dialysis, needs to be applied. Considering centrifugation may not always precipitate all of the NPs, ultrafiltration through 2 KDa membrane was used in this study. However, unlike other metal ions (such as Zn and Fe), Ag^+ ions form insoluble compounds such as silver oxide, silver chloride and silver sulfide in cell culture media (SI, Fig 5S), this causes loss of free Ag^+ ions in the solution and therefore affects the ICP-OES results and interpretation of the dissolution rates. In addition, the potential adsorption/co-adsorption of biomolecule and metal ions on to the filter should be taken into account, and may lead to small level of Ag loss during sample preparation. The limitation of using ICP-OES to study the kinetics of Ag^+ dissolution in cell culture media was further demonstrated by a control experiment, in which, ICP-OES was used to determine the amount of free Ag^+ ions from a known concentration of $AgNO_3$ added to both DI-water and three cell media solutions, incubated at 37 °C for 0.5 h. Fig. 3b shows that 100 % of free Ag^+ ions were detected in the $AgNO_3$ DI-water solution. In contrast, the amount of solubilized sivler in the cell media was less than 0.5 μg/mL after incubation, despite using the same starting concentration of Ag^+ ions, *i.e.* the dissolved Ag^+ ions are sequestered as insoluble precipitates in the cell media. The negligible solubilized silver was detected in DI-water incubated with AgNWs at37 °C up to one week (Fig3a), indicates extremely slow oxidation dissolution rate of AgNWs. The time resolved pH measurements of DMEM and PRMI-1640 incubated with AgNWs respectively were also carried out for Ag dissolution rate study. However, possibly due to the slow reaction rate, low reactant concentration and high buffer capacity of cell media,[41] no significant pH variations were detected, see SI, Fig 6S.

Since the AgNWs were only sulfidized in the DCCM-1 cell culture medium, the effects of the medium components were considered. The complete formulation of DCCM-1 is confidential and so identifying the exact species involved in the sulfidation process was difficult. Therefore, the medium was separated into two fractions using ultra-centrifugal filtration with a 3 KDa pore size filter membrane: this separation process allows

discrimination between the small molecule solutes and salts and the proteins, in terms of the formation of Ag_2S on reaction with the AgNWs. This experiment may also provide vital clues about whether sulfur rich proteins are likely to transform AgNWs in the lung. For example, there are four types of lung surfactant proteins present in the lung. And some of these (e.g. SPA, ,SPB and SPD) contain sulphur,[43]. The AgNPs may interact strongly with lung proteins, potentially affecting function, and in turn these proteins might alter the chemistry of Ag NPs. The extracted proteins were dispersed in phosphate buffered saline (PBS), in which AgNWs proved to be stable (Fig. 5a). However, after 6 hours of incubation in the small molecule solutes and salts component of DCCM-1, small crystals had formed on the nanowire surface (Fig. 4a). The resulting morphology resembled that of AgNWs incubated in whole DCCM-1 (Fig. 2a), but since the incubation time was longer in this case, the extent of crystal formation was much larger. The spacing between the spots in the SAED pattern (inset Fig. 4a) corresponded with lattice spacings of 0.313 ± 0.010, 0.288 ± 0.009, 0.264 ± 0.008 and 0.250 ± 0.008 nm. These values were consistent with the (111), (−112), (−121) and (022) lattice spacings of monoclinic Ag_2S, respectively (Ref. #00-014-0072). HRTEM analysis (Fig. 4b) indicated that the interplanar spacing measured from the surface of the nanowires were 0.250 ± 0.008 nm and 0.280 ± 0.008 nm, which was consistent with the (112) and (−112) interplanar spacing of Ag_2S, respectively (Ref. #00-014-0072). More HRTEM results are represented in SI, Fig 7S and 8S. These findings suggest that the AgNWs have undergone a sulfidation process, whereby a thin layer of Ag_2S nanocrystals has formed on the surface of the original NWs. The peak at 2.31 keV in the EDX spectrum collected from the surface of the AgNWs (Fig. 4c-bottom), corresponds to the S(Kα) peak. A STEM-EDX line profile scanned across the AgNW is shown in SI-Fig. 9S. A similar transformation, however, was not observed when AgNWs were incubated with proteins extracted from DCCM-1 (Fig. 4d). The morphology of the AgNWs has not changed and the crystal lattice spacings, measured both at the core and the surface of the AgNWs (Fig. 4e), were consistent with the (111) interplanar spacing of bulk Ag (Ref. # 01-087-0597). EDX spectra collected from the AgNWs also failed to detect the presence of sulfur (Fig. 4f and SI, Fig. 10S). The above observations indicate that small molecule solutes and salts, but not proteins contained in DCCM-1, were responsible for the AgNW sulfidation. The ICP-OES study monitoring the sulfur content in DMEM, RPMI-1640 and DCCM-1 filtrate was also carried out. RPMI-1640 and DMEM contain many inorganic salts, amino acids and other small molecule solutes (Table S2). $MgSO_4$, cystine, methionine and HEPES (2-[4-(2-hydroxyethyl)piperazin-1-yl]ethanesulfonic acid, a buffer agent) are sulfur containing components in those two cell media. No substantial sulfur content change was detected in DMEM (SI, Fig 11Sa), which supports the TEM results, and further confirmed sulfate and sulfur containing amino acids do not lead to sulfidation. Similar observation was also suggested in Liu et al's study,[44] that sulfate and sulfite do not react with AgNPs. The RPMI has a much higher sulfur concentration than DMEM (~220 ppm) (SI, Fig 11Sb), this is due to the relative high concentration of HEPES content which provides an extra buffering effect. Due to this reason, the detection of small sulfur variations (0.65 – 6.5 μg/mL for 100 % sulfidise 5 and 50 μg/mL AgNWs respectively) may be difficult for ICP-OES. The sulfur concentration in DCCM-1 filtrates (containing small molecule solutes and salts) is about 115 ppm (SI, Fig 11Sc). The cell medium possible contains not only silver reactive sulfur species, but also possibly contain sulfate and sulfur containing small molecules, those are

common components used in other cell media but no reactive with silver. Fig 1c shows there was no significant change of sulfur concentration over 24 h incubation time for both 5 and 50 μg/mL AgNWs groups. However, this does not necessary mean that there was no sulfidation reaction. For example, even if the sulfur concentration is in the range of a few ppm or even lower can lead to significant sulfidation which can be easily observed by high resolution electron microscope technique, however, may not be detectable by ICP-OES. It can be estimated that, for 5 μg/mL AgNWs (3 μm in length, 130 nm in diameter), only 0.1 μg/mL (ppm) sulfur is needed to complete AgNWs surface sulfidation of 10 nm in thickness. This surface morphology change can be easily characterized by HRTEM (Fig 4a), however, the reduction of 0.1 ppm sulfur may not be easily identified by ICP-OES especially in a system with a high sulfur background concentration.

In order to study the effect of sulfur containing amino acids and proteins on the AgNWs, samples were incubated with cysteine and BSA dispersed in PBS. As a control, the stability of AgNWs in PBS medium was tested and no transformation was observed (Fig. 5a). HAADF-STEM imaging (Fig. 5b–c top) showed that the morphology of the AgNWs had not changed after 6 h of incubation in both cysteine and BSA, while EDX analysis (Fig. 5b–c bottom) did not detect the presence of any sulfur. These results were further supported by HRTEM analysis (SI, Fig 12S) Taken together, these findings show that neither cysteine nor BSA sulfidize the AgNWs in this experiment, in contrast to recent work that suggested the surface coating of Ag nanoplates by cysteine-HCl[45].

The sulfidation of the AgNWs may occur via two chemical reactions:

1. a direct route (particle-fluid reaction), indicated by reaction equations (1a–c), which depends on the sulfide concentration, such that the reaction rate accelerates as the sulfide concentration increases.

$$4Ag + O_2 + 2H_2S \rightarrow 2Ag_2S + 2H_2O \quad (1a)$$

$$4Ag + O_2 + 2HS^- \rightarrow 2Ag_2S + 2OH^- \quad (1b)$$

$$4Ag + O_2 + 4H^+ \rightarrow 2S^{2-} \rightarrow 2Ag_2S + 2H_2O \quad (1c)$$

2. an in-direct route, *i.e.* oxidative dissolution of silver followed by sulfide precipitation (reaction equation 2a–d), which is effectively independent of sulfide concentration (because the K_{sp} of Ag_2S is so low), but determined by the oxidative dissolution rate of silver[44].

$$2Ag + \frac{1}{2}O_2 + 2H^+ \rightarrow 2Ag^+ + H_2O \quad (2a)$$

$$2Ag^+ + H_2S \rightarrow Ag_2S + 2H^+ \quad (2b)$$

$$2Ag^{+}+HS^{-} \rightarrow Ag_2S+H^{+} \quad (2c)$$

$$2Ag^{+}+S^{2-} \rightarrow Ag_2S \quad (2d)$$

The silver sulfidation is a complex process and involves the competition of these two sulfidation pathways, which is dependent on the sulfide concentration in the environment. A model of 30 nm AgNPs oxysulfidation over a wide range of sulfide concentrations proposed by Liu et al,[44] suggested that below sulfide concentration 0.025 ppm, the sulfidation is dominated by the indirect pathway. The indirect sulfidation rate is independent of sulfide concentration, and only limited by oxidation dissolution rate (reaction 2a). The indirect process is a relatively slow process, the reaction half-life of 30 nm AgNPs sulfidation is about 10–20 days. Above 0.025 ppm sulfide, the mechanism becomes direct sulfidation dominated. The direct sulfidation is a relatively fast process even at low sulfide concentrations, for example, the reaction half-life is about 2 days under a 0.1 ppm sulfide concentration, and the reaction half-life is shorten to 0.1–0.2 days in a 1 ppm sulfide condition. Fig 6a-right shows the AgNWs morphology incubated in DCCM-1 for only 0.25 h (15 min). The presence of the PVP coating on the surface of sulfidized AgNWs, suggests a direct sulfidation-dominated process at the early stage of the incubation process, i.e. the sulfide ions diffused through PVP coating that initiated sulfidation on the AgNWs surface. This is hypothesis is likely to be true, based on the kinetics of indirect and direct sulfidation pathways. Within such a short time (0.25 h), there will be hardly any Ag^{+} ions forming by oxidative dissolution, as indicated by extremely low AgNWs dissolution rate, as supported by the dissolution study in water (Figure 3). Furthermore, our recently publication also suggested a very slow oxidation dissolution rate even for 20 nm AgNPs, which should have a higher reactivity than AgNWs (130 nm in diameter, > 2.8 μm in length) studied here. In that study, only ~0.4 % of Ag ions were measured after 14 days incubation of 20 nm AgNPs at pH 7.[46] Further sulfidation of the wires along both long and short axis of NWs was observed after 6 h of incubation (Fig. 6b-left). Complete sulfidation on the tips of the wires, indicates a faster sulfidation rate at the tips along the long axis, this is likely due to the difference of surface energy of {111} and {100} facets and the different binding energy of PVP to these facets. The end of AgNWs were terminated by {111} facets and the side surfaces are bounded by {100} facets. The lower surface energy of {111} facets than {100} facets, and the weaker binding of PVP to {111} than {100} facets contribute to a higher reactivity at the AgNWs tips positions than side surfaces.[38]. The transformation of AgNWs to Ag_2S was further confirmed by acquiring S and Ag STEM-EDX maps from the boxed region close to the end of the AgNWs (Fig. 6b-right). The STEM-EDX mapping showing a structure with a more sulfur abundant surface and a silver rich core, suggests a surface sulfidation process. In contrast, complete sulfidiation of AgNWs of smaller diameters was also observed (SI, Fig 14S). After 24 h, hollowed-out structures were found in some AgNWs as indicated by arrows (Fig. 6c). The hollow structures could attribute to both direct and indirect sulfidation. As direct pathway, metal ions transported from the inner part of a Ag particle through a sulfidized (oxidized) layer(s), and form silver sulfide on the surface of particle. On the other hand, the in-direct sulfidation may also play a part in the sulfidation

process, especially at the later stage of incubation. As long as the sulfide species are continuously consumed, the direct sulfidation rate decreases, and, at some certain point, the in-direct sulfidation starts to become dominated. The dissolved silver could have possibly precipitated on existing sulfide crystals or diffused out through the PVP capping layer. A similar sulfidation pattern for AgNPs was also observed (SI, Fig 15S).

In summary, crystalline Ag_2S formed on AgNWs surface within 1 hour of incubation in DCCM-1, likely *via* a direct sulfidation (particle-fluid reaction) initiated transformation. In contrast, the AgNWs did not change their chemistry in RPMI-1640 or DMEM. When the DCCM-1 cell culture medium was separated into its small molecule solutes and salts and protein components, the AgNWs sulfidized in the fraction containing small molecule solutes and salts, but not in the protein fraction. These results correlate with other reports which have demonstrated the sulfidation of PVP-coated AgNWs upon exposure to ambient atmosphere and the formation of a thin layer of Ag_2S nanocrystals on their surface[47, 48]. An analysis of field samples from water treatment plants has also revealed the presence of Ag_2S nanocrystals, suggesting that AgNPs that enter wastewater streams are sulfidized[49]. AgNPs have been shown to react with dissolved sulfide species in water and the reaction mechanism depends on the sulfide concentration[50]. Due to the low solubility of Ag_2S, this transformation largely limits the amount of free Ag^+ ions[51] and is therefore likely to affect the bioreactivity of the AgNWs, at least in terms of short term cytotoxicity. Indeed, the presence of sulfide *reduced* the toxicity of Ag to Daphnia magna by more than a 5-fold[52] and to nitrifying bacteria by up to 80%[53]. Moreover, 9 nm Ag_2S nanoparticles were found not to be cytotoxic to Gram-positive and Gram-negative bacteria or eukaryotic cell lines[54]. It is known that sulfide species, such as H_2S, HS^- and S^{2-}, exist in all human tissues, the total concentration of which is in the order of μM[55–57]. The Ag sulfidation mechanism in cell culture medium suggested in this study provides insights on a possible Ag degradation mechanism *in vivo* through the sulfidation pathway, which likely to affect the bioreactivity and therefore the toxicity of Ag nanomaterials. Indeed, the silver sulfidation as a potential detoxification mechanism has been observed in a vitro study on lung epithelial cells and reported by us very recently. As *in vivo*, the formation of argyrial silver sulphide formed by partial dissolution in the GI tract followed by ion uptake, systemic circulation has been reported,[35], however, to fully understand the transformation kinetics in different *in vivo* conditions much more information is needed, especially to the time of the study and lifetime of the system being examined.Reports have shown that Ag^+ ions can bind strongly to both inorganic sulfur groups as well as organosulfur compounds, with the highest affinity for thiols such as cysteine[58]. The PVP capped AgNWs in this work did not sulfidize in the presence of BSA or cysteine alone. Ag^+ ions may have a high affinity for thiols and cysteine, changing their biological activity, however Ag^+ ions may not be able to remove sulfur from biological molecules to form an inorganic sulfide without the existence of other oxidising species. Our study highlights that the effects of exposure of AgNWs to the environment should be considered to ensure that the AgNWs do not transform in the environment prior to or during incubation with the cell culture media or cells, unless studying specific effects of extracellular fluids on the particle-cell interaction and bioreactivity. We managed to identify the small molecule solutes and salts in DCCM rather than proteins are responsible for sulfidation, however, as the media composition is

confidential and complex we were not able to identify the specific component(s). However, the main aim of this study, is to emphasize the importance of appropriate media and material control in order to allow accurate predictions about Ag toxicity, as the complex of cell media or other physiological solutions. Passing this message, seems to be important and timely, as currently there is massive amount of Ag toxicity research undergoing, however much less attention has been paid to study the stability of Ag materials in various physiological solutions which may affect the accurate prediction of silver toxicity outcome.

Supplementary Material

Refer to Web version on PubMed Central for supplementary material.

Acknowledgments

This work was funded in part by a grant from the NIEHS (grant number U19ES019536) and the US EPA/NERC (EPA STAR RD83469301 and NERC). AP acknowledges an ERC starting grant (Project number 257182) for additional support for AP, AEG and SC and for support with the electron microscopy characterisation. We thank Mr. Henock Solomon of USC for his administrative assistance.

References

1. Wijnhoven SWP, Peijnenburg W, Herberts CA, Hagens WI, Oomen AG, Heugens EHW, Roszek B, Bisschops J, Gosens I, Van de Meent D, Dekkers S, De Jong WH, Van Zijverden M, Sips A, Geertsma RE. Nano-silver - a review of available data and knowledge gaps in human and environmental risk assessment. Nanotoxicology. 2009; 3(2) 109-U78.
2. Chen X, Schluesener HJ. Nanosilver: A nanoproduct in medical application. Toxicology Letters. 2008; 176(1):1–12. [PubMed: 18022772]
3. Marambio-Jones C, Hoek EMV. A review of the antibacterial effects of silver nanomaterials and potential implications for human health and the environment. Journal of Nanoparticle Research. 2010; 12(5):1531–1551.
4. Hansen SF, Baun A. When enough is enough. Nature Nanotechnology. 2012; 7(7):409–411.
5. Eturska M, Obreshkova E. Argyria in the prolonged use of adsorgan. Vutreshni bolesti. 1979; 18(2): 121–123. [PubMed: 462932]
6. Spencer WH, Garron LK, Contreras F, Hayes TL, Lai C. Endogenous and exogenous ocular and systemic silver deposition. Transactions of the ophthalmological societies of the United Kingdom. 1980; 100(Pt 1):171–178. [PubMed: 6943824]
7. Fabrega J, Luoma SN, Tyler CR, Galloway TS, Lead JR. Silver nanoparticles: Behaviour and effects in the aquatic environment. Environment International. 2011; 37(2):517–531. [PubMed: 21159383]
8. Foldbjerg R, Dang DA, Autrup H. Cytotoxicity and genotoxicity of silver nanoparticles in the human lung cancer cell line, A549. Archives of toxicology. 2011; 85(7):743–750. [PubMed: 20428844]
9. Park MV, Neigh AM, Vermeulen JP, de la Fonteyne LJ, Verharen HW, Briede JJ, van Loveren H, de Jong WH. The effect of particle size on the cytotoxicity, inflammation, developmental toxicity and genotoxicity of silver nanoparticles. Biomaterials. 2011; 32(36):9810–9817. [PubMed: 21944826]
10. Costa CS, Ronconi JV, Daufenbach JF, Goncalves CL, Rezin GT, Streck EL, Paula MM. In vitro effects of silver nanoparticles on the mitochondrial respiratory chain. Molecular and cellular biochemistry. 2010; 342(1–2):51–56. [PubMed: 20411305]
11. Suresh AK, Pelletier DA, Wang W, Morrell-Falvey JL, Gu B, Doktycz MJ. Cytotoxicity induced by engineered silver nanocrystallites is dependent on surface coatings and cell types. Langmuir : the ACS journal of surfaces and colloids. 2012; 28(5):2727–2735. [PubMed: 22216981]

12. Kim HR, Kim MJ, Lee SY, Oh SM, Chung KH. Genotoxic effects of silver nanoparticles stimulated by oxidative stress in human normal bronchial epithelial (BEAS-2B) cells. Mutation research. 2011; 726(2):129–135. [PubMed: 21945414]
13. Stoehr LC, Gonzalez E, Stampfl A, Casals E, Duschl A, Puntes V, Oostingh GJ. Shape matters: effects of silver nanospheres and wires on human alveolar epithelial cells. Particle and fibre toxicology. 2011; 8:36. [PubMed: 22208550]
14. Arora S, Jain J, Rajwade JM, Paknikar KM. Cellular responses induced by silver nanoparticles: In vitro studies. Toxicology letters. 2008; 179(2):93–100. [PubMed: 18508209]
15. Kang K, Jung H, Lim JS. Cell Death by Polyvinylpyrrolidine-Coated Silver Nanoparticles is Mediated by ROS-Dependent Signaling. Biomolecules & Therapeutics. 2012; 20(4):399–405. [PubMed: 24009827]
16. Piao MJ, Kang KA, Lee IK, Kim HS, Kim S, Choi JY, Choi J, Hyun JW. Silver nanoparticles induce oxidative cell damage in human liver cells through inhibition of reduced glutathione and induction of mitochondria-involved apoptosis. Toxicology letters. 2011; 201(1):92–100. [PubMed: 21182908]
17. AshaRani PV, Mun GLK, Hande MP, Valiyaveettil S. Cytotoxicity and Genotoxicity of Silver Nanoparticles in Human Cells. Acs Nano. 2009; 3(2):279–290. [PubMed: 19236062]
18. Dibrov P, Dzioba J, Gosink KK, Hase CC. Chemiosmotic mechanism of antimicrobial activity of Ag+ in Vibrio cholerae. Antimicrobial Agents and Chemotherapy. 2002; 46(8):2668–2670. [PubMed: 12121953]
19. Holt KB, Bard AJ. Interaction of Silver(I) Ions with the Respiratory Chain of Escherichia coli: An Electrochemical and Scanning Electrochemical Microscopy Study of the Antimicrobial Mechanism of Micromolar Ag+ Biochemistry. 2005; 44(39):13214–13223. [PubMed: 16185089]
20. Lok C-N, Ho C-M, Chen R, He Q-Y, Yu W-Y, Sun H, Tam PK-H, Chiu J-F, Che C-M. Proteomic Analysis of the Mode of Antibacterial Action of Silver Nanoparticles. Journal of Proteome Research. 2006; 5(4):916–924. [PubMed: 16602699]
21. Stohs SJ, Bagchi D. Oxidative mechanisms in the toxicity of metal ions. Free Radical Biology and Medicine. 1995; 18(2):321–336. [PubMed: 7744317]
22. Carlson C, Hussain SM, Schrand AM, K. Braydich-Stolle L, Hess KL, Jones RL, Schlager JJ. Unique Cellular Interaction of Silver Nanoparticles: Size-Dependent Generation of Reactive Oxygen Species. The Journal of Physical Chemistry B. 2008; 112(43):13608–13619. [PubMed: 18831567]
23. Morones JR, Elechiguerra JL, Camacho A, Holt K, Kouri JB, Ramirez JT, Yacaman MJ. The bactericidal effect of silver nanoparticles. Nanotechnology. 2005; 16(10):2346–2353. [PubMed: 20818017]
24. Yang X, Gondikas AP, Marinakos SM, Auffan M, Liu J, Hsu-Kim H, Meyer JN. Mechanism of silver nanoparticle toxicity is dependent on dissolved silver and surface coating in Caenorhabditis elegans. Environmental science & technology. 2012; 46(2):1119–1127. [PubMed: 22148238]
25. Xiu ZM, Zhang QB, Puppala HL, Colvin VL, Alvarez PJJ. Negligible Particle-Specific Antibacterial Activity of Silver Nanoparticles. Nano Lett. 2012; 12(8):4271–4275. [PubMed: 22765771]
26. Navarro E, Piccapietra F, Wagner B, Marconi F, Kaegi R, Odzak N, Sigg L, Behra R. Toxicity of Silver Nanoparticles to Chlamydomonas reinhardtii. Environmental science & technology. 2008; 42(23):8959–8964. [PubMed: 19192825]
27. Choi O, Hu ZQ. Size dependent and reactive oxygen species related nanosilver toxicity to nitrifying bacteria. Environmental science & technology. 2008; 42(12):4583–4588. [PubMed: 18605590]
28. Fabrega J, Fawcett SR, Renshaw JC, Lead JR. Silver Nanoparticle Impact on Bacterial Growth: Effect of, pH, Concentration, and Organic Matter. Environmental science & technology. 2009; 43(19):7285–7290. [PubMed: 19848135]
29. Yin LY, Cheng YW, Espinasse B, Colman BP, Auffan M, Wiesner M, Rose J, Liu J, Bernhardt ES. More than the Ions: The Effects of Silver Nanoparticles on Lolium multiflorum. Environmental science & technology. 2011; 45(6):2360–2367. [PubMed: 21341685]

30. Xiu ZM, Ma J, Alvarez PJ. Differential effect of common ligands and molecular oxygen on antimicrobial activity of silver nanoparticles versus silver ions. Environmental science & technology. 2011; 45(20):9003–9008. [PubMed: 21950450]
31. Liu J, Sonshine DA, Shervani S, Hurt RH. Controlled Release of Biologically Active Silver from Nanosilver Surfaces. Acs Nano. 2010; 4(11):6903–6913. [PubMed: 20968290]
32. Graedel TE, Franey JP, Gualtieri GJ, Kammlott GW, Malm DL. On the Mechanism of Silver and Copper Sulfidation by Atmospheric H2s and Ocs. Corrosion Science. 1985; 25(12):1163–1180.
33. Franey JP, Kammlott GW, Graedel TE. The Corrosion of Silver by Atmospheric Sulfurous Gases. Corrosion Science. 1985; 25(2):133–143.
34. Levard C, Hotze EM, Lowry GV, Brown GE Jr. Environmental transformations of silver nanoparticles: impact on stability and toxicity. Environmental science & technology. 2012; 46(13): 6900–6914. [PubMed: 22339502]
35. Liu J, Wang Z, Liu FD, Kane AB, Hurt RH. Chemical transformations of nanosilver in biological environments. Acs Nano. 2012; 6(11):9887–9899. [PubMed: 23046098]
36. Chen S, Goode AE, Sweeney S, Theodorou IG, Thorley AJ, Ruenraroengsak P, Chang Y, Gow A, Schwander S, Skepper J, Zhang JJ, Shaffer MS, Chung KF, Tetley TD, Ryan MP, Porter AE. Sulfidation of silver nanowires inside human alveolar epithelial cells: a potential detoxification mechanism. Nanoscale. 2013; 5(20):9839–9847. [PubMed: 23970174]
37. Sun Y, Xia Y. Large-Scale Synthesis of Uniform Silver Nanowires Through a Soft, Self-Seeding, Polyol Process. Advanced Materials. 2002; 14(11):833–837.
38. Xia Y, Xiong Y, Lim B, Skrabalak SE. Shape-controlled synthesis of metal nanocrystals: simple chemistry meets complex physics? Angew Chem Int Ed Engl. 2009; 48(1):60–103. [PubMed: 19053095]
39. Muller KH, Kulkarni J, Motskin M, Goode A, Winship P, Skepper JN, Ryan MP, Porter AE. pH-Dependent Toxicity of High Aspect Ratio ZnO Nanowires in Macrophages Due to Intracellular Dissolution. Acs Nano. 2010; 4(11):6767–6779. [PubMed: 20949917]
40. Chen S, Wang LJ, Duce SL, Brown S, Lee S, Melzer A, Cuschieri SA, Andre P. Engineered Biocompatible Nanoparticles for in Vivo Imaging Applications. J Am Chem Soc. 2010; 132(42): 15022–15029. [PubMed: 20919679]
41. Acker H, Carlsson J, Holtermann G, Nederman T, Nylen T. Influence of glucose and buffer capacity in the culture medium on growth and pH in spheroids of human thyroid carcinoma and human glioma origin. Cancer Research. 1987; 47(13):3504–3508. [PubMed: 3581085]
42. McGilvery CM, Goode AE, Shaffer MSP, McComb DW. Contamination of holey/lacey carbon films in STEM. Micron. 2012; 43(2–3):450–455. [PubMed: 22192979]
43. Kuroki Y, Voelker DR. Pulmonary surfactant proteins. J Biol Chem. 1994; 269(42):25943–25946. [PubMed: 7929300]
44. Liu JY, Pennell KG, Hurt RH. Kinetics and Mechanisms of Nanosilver Oxysulfidation. Environmental science & technology. 2011; 45(17):7345–7353. [PubMed: 21770469]
45. George S, Lin SJ, Jo ZX, Thomas CR, Li LJ, Mecklenburg M, Meng H, Wang X, Zhang HY, Xia T, Hohman JN, Lin S, Zink JI, Weiss PS, Nel AE. Surface Defects on Plate-Shaped Silver Nanoparticles Contribute to Its Hazard Potential in a Fish Gill Cell Line and Zebrafish Embryos. Acs Nano. 2012; 6(5):3745–3759. [PubMed: 22482460]
46. Leo BF, Chen S, Kyo Y, Herpoldt KL, Terrill NJ, Dunlop IE, McPhail DS, Shaffer MS, Schwander S, Gow A, Zhang J, Chung KF, Tetley TD, Porter AE, Ryan MP. The Stability of Silver Nanoparticles in a Model of Pulmonary Surfactant. Environmental science & technology. 2013; 47(19):11232–11240. [PubMed: 23988335]
47. Fu X, Zou H, Zhou L. A Novel Synthesis Route of Ag₂S Nanotubes by Sulfidizing Silver Nanowires in Ambient Atmosphere. Journal of Nanoscience and Nanotechnology. 2010; 10(9):5851–5856. [PubMed: 21133115]
48. Elechiguerra JL, Larios-Lopez L, Liu C, Garcia-Gutierrez D, Camacho-Bragado A, Yacaman MJ. Corrosion at the nanoscale: The case of silver nanowires and nanoparticles. Chemistry of Materials. 2005; 17(24):6042–6052.

49. Kim B, Park C-S, Murayama M, Hochella MF Jr. Discovery and Characterization of Silver Sulfide Nanoparticles in Final Sewage Sludge Products. Environmental science & technology. 2010; 44(19):7509–7514. [PubMed: 20839838]
50. Liu J, Pennell KG, Hurt RH. Kinetics and mechanisms of nanosilver oxysulfidation. Environmental science & technology. 2011; 45(17):7345–7353. [PubMed: 21770469]
51. Levard C, Reinsch BC, Michel FM, Oumahi C, Lowry GV, Brown GE. Sulfidation processes of PVP-coated silver nanoparticles in aqueous solution: impact on dissolution rate. Environmental science & technology. 2011; 45(12):5260–5266. [PubMed: 21598969]
52. Bianchini A, Bowles KC, Brauner CJ, Gorsuch JW, Kramer JR, Wood CM. Evaluation of the effect of reactive sulfide on the acute toxicity of silver (I) to Daphnia magna, part 2: Toxicity results. Environmental Toxicology and Chemistry. 2002; 21(6):1294–1300. [PubMed: 12069317]
53. Choi O, Clevenger TE, Deng B, Surampalli RY, Ross L Jr, Hu Z. Role of sulfide and ligand strength in controlling nanosilver toxicity. Water research. 2009; 43(7):1879–1886. [PubMed: 19249075]
54. Suresh AK, Doktycz MJ, Wang W, Moon JW, Gu B, Meyer HM 3rd, Hensley DK, Allison DP, Phelps TJ, Pelletier DA. Monodispersed biocompatible silver sulfide nanoparticles: facile extracellular biosynthesis using the gamma-proteobacterium, Shewanella oneidensis. Acta biomaterialia. 2011; 7(12):4253–4258. [PubMed: 21798382]
55. Furne J, Saeed A, Levitt MD. Whole tissue hydrogen sulfide concentrations are orders of magnitude lower than presently accepted values. American Journal of Physiology-Regulatory Integrative and Comparative Physiology. 2008; 295(5):R1479–R1485.
56. Li L, Rose P, Moore PK. Hydrogen Sulfide and Cell Signaling. Annual Review of Pharmacology and Toxicology, vol 51, 2011. 2011; 51:169–187.
57. Perry MM, Hui CK, Whiteman M, Wood ME, Adcock I, Kirkham P, Michaeloudes C, Chung KF. Hydrogen sulfide inhibits proliferation and release of IL-8 from human airway smooth muscle cells. American Journal of Respiratory Cell and Molecular Biology. 2011; 45(4):746–752. [PubMed: 21297080]
58. Bell RA, Kramer JR. Structural chemistry and geochemistry of silver-sulfur compounds: Critical review. Environmental Toxicology and Chemistry. 1999; 18(1):9–22.

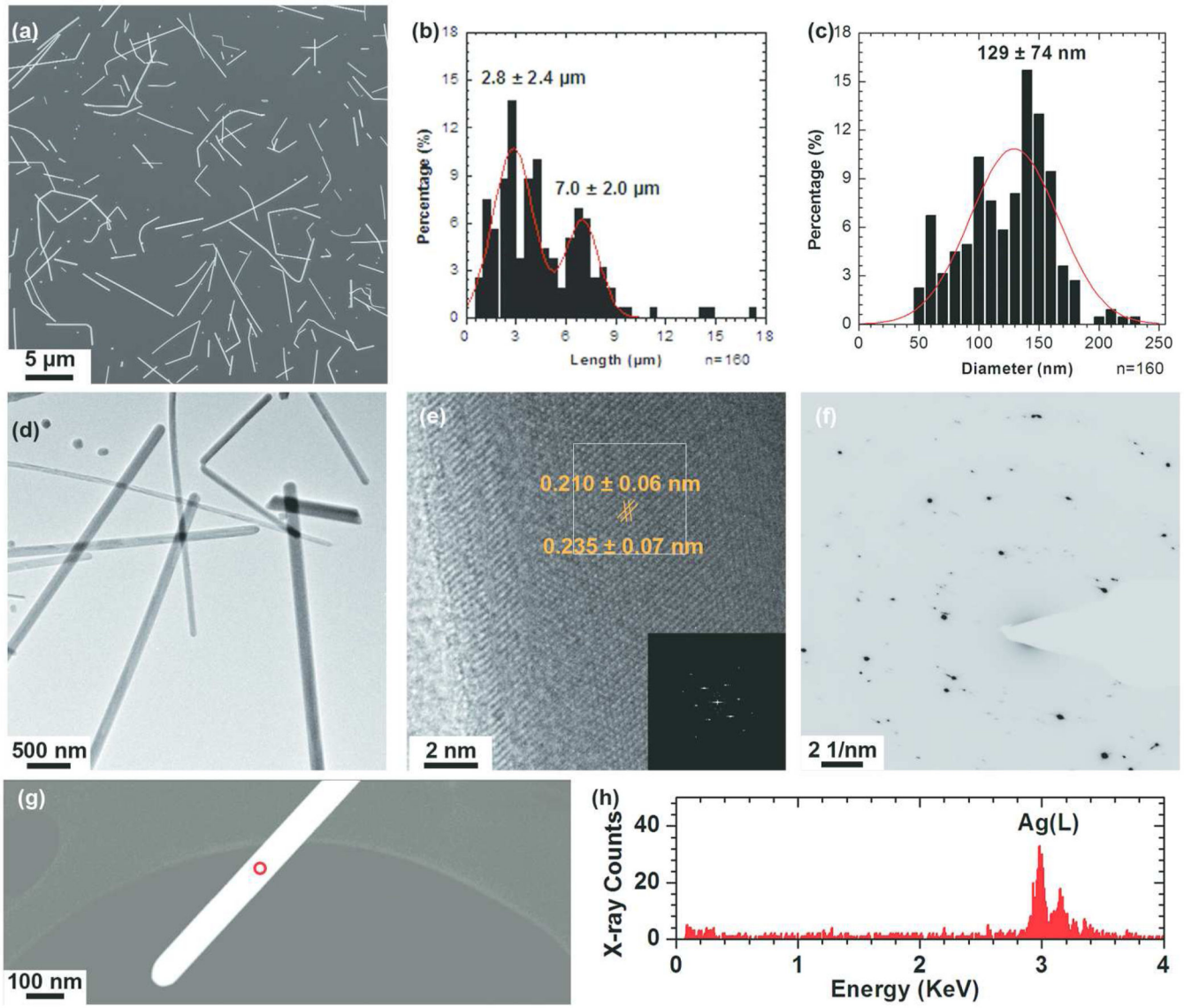

Figure 1.

Physicochemical characterization of as-synthesized AgNWs by SEM, TEM and SAED. (a) SEM image of as-synthesized AgNWs and their (b) length and (c) diameter distribution. The curves represent the Gaussian fit to the data. (d) A low-resolution bright field (BF) TEM image of the AgNWs. (e) A high-resolution BF-TEM image of a single AgNW, revealing its crystal structure. The inset is the corresponding FFT pattern taken from the boxed area. (f) SAED pattern taken from a region containing several AgNWs, using a selected area aperture size of ~560 nm. (g) HAADF-STEM image of a single AgNW and (h) the corresponding EDX spectrum taken from the area circled in (g). The two peaks at 2.98 keV and 3.15 keV correspond to the Ag(L_α) and Ag(L_β) peaks respectively.

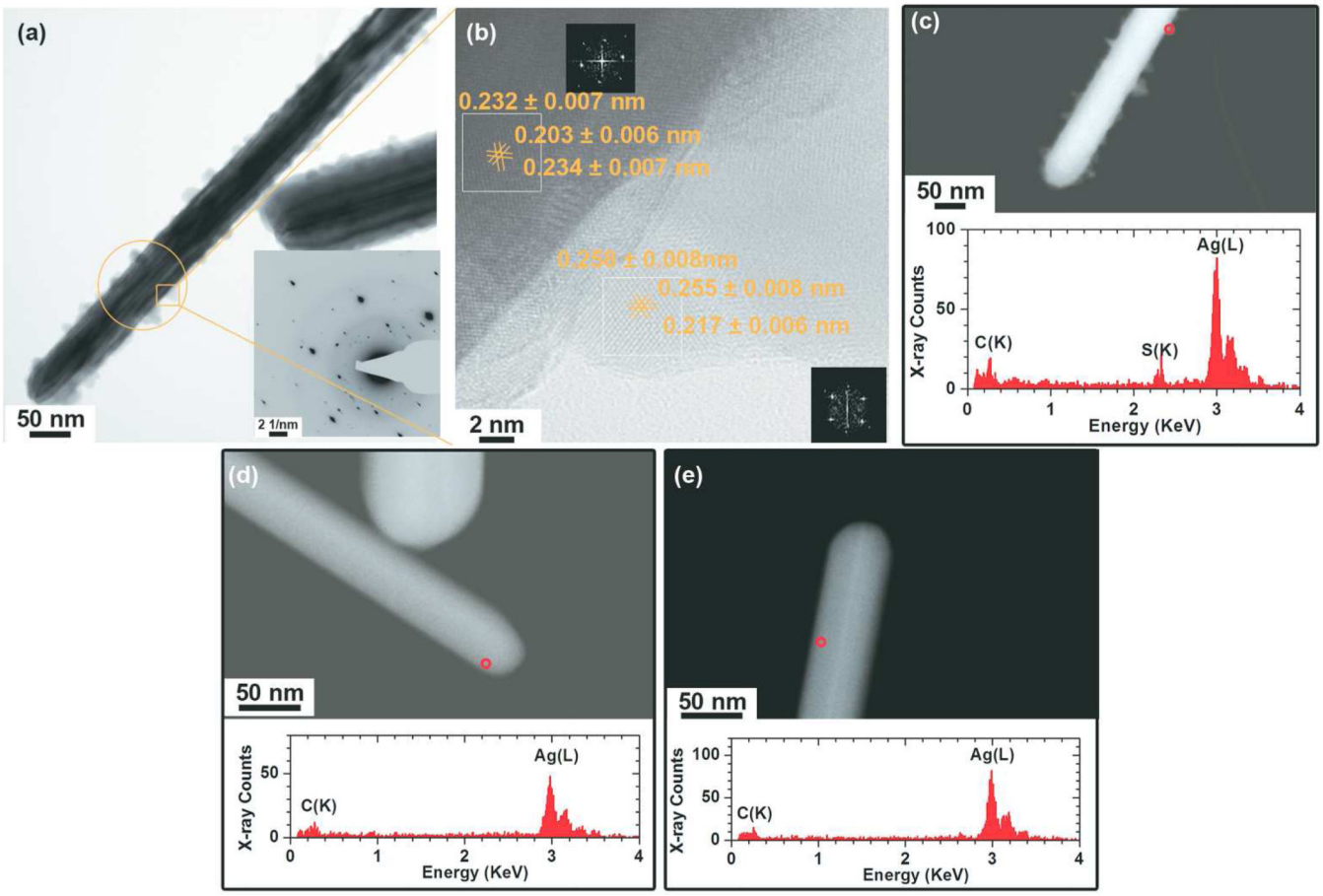

Figure 2.

Physicochemical characterization of AgNWs incubated in various cell culture media, for 1h at 37 °C: (a–c) DCCM-1, (d) DMEM and (e) RPMI-1640. (a) A representative BF-TEM image of the AgNWs incubated in DCCM-1 medium, showing the formation of crystallites on the surface of the AgNWs. The inset is a SAED pattern taken from the circled area (aperture size ~130 nm). (b) An HRTEM image collected from the boxed area in Fig. 2a reveals that the crystallites have a different crystal structure than the original AgNWs. The insets are FFT patterns taken from the two boxed areas. HAADF-STEM image (c-top) taken from the same area as Fig. 2a. STEM-EDX spectra were collected from the circled area (c-bottom). (d–e) HAADF-STEM images (top) and EDX spectra (bottom) of AgNWs incubated in DMEM and RPMI-1640 cell media, respectively.

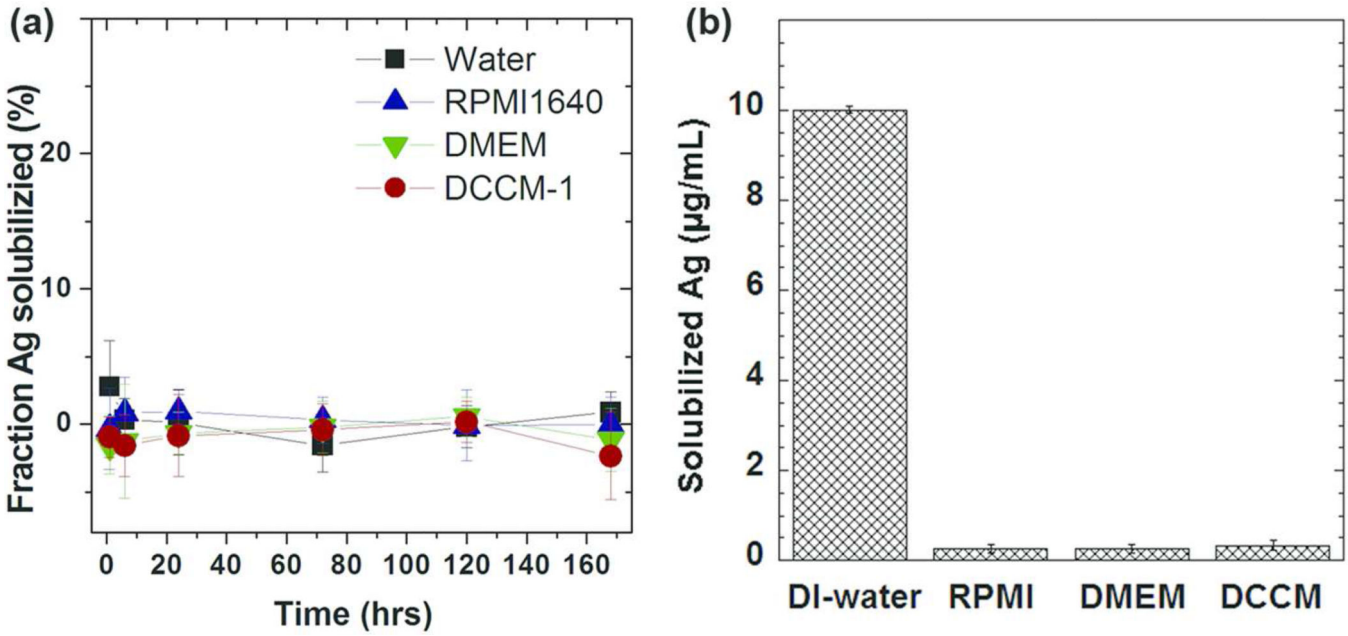

Figure 3.

(a) The kinetics of AgNWs dissolution following incubation of the Ag NWs in DI-water, RPMI-1640, DMEM and DCCM-1 at 37 °C. The solubilized silver concentrations were measured by ICP-OES from 1 h up to 168 h. (b) ICP-OES analysis of solubilized silver concentrations of 17.0 μg/mL $AgNO_3$ (equal to an Ag concentration of 10 μg/mL) in DI-water, RPMI-1640, DMEM and DCCM-1 solutions, incubated at 37 °C for 0.5 h (n = 3).

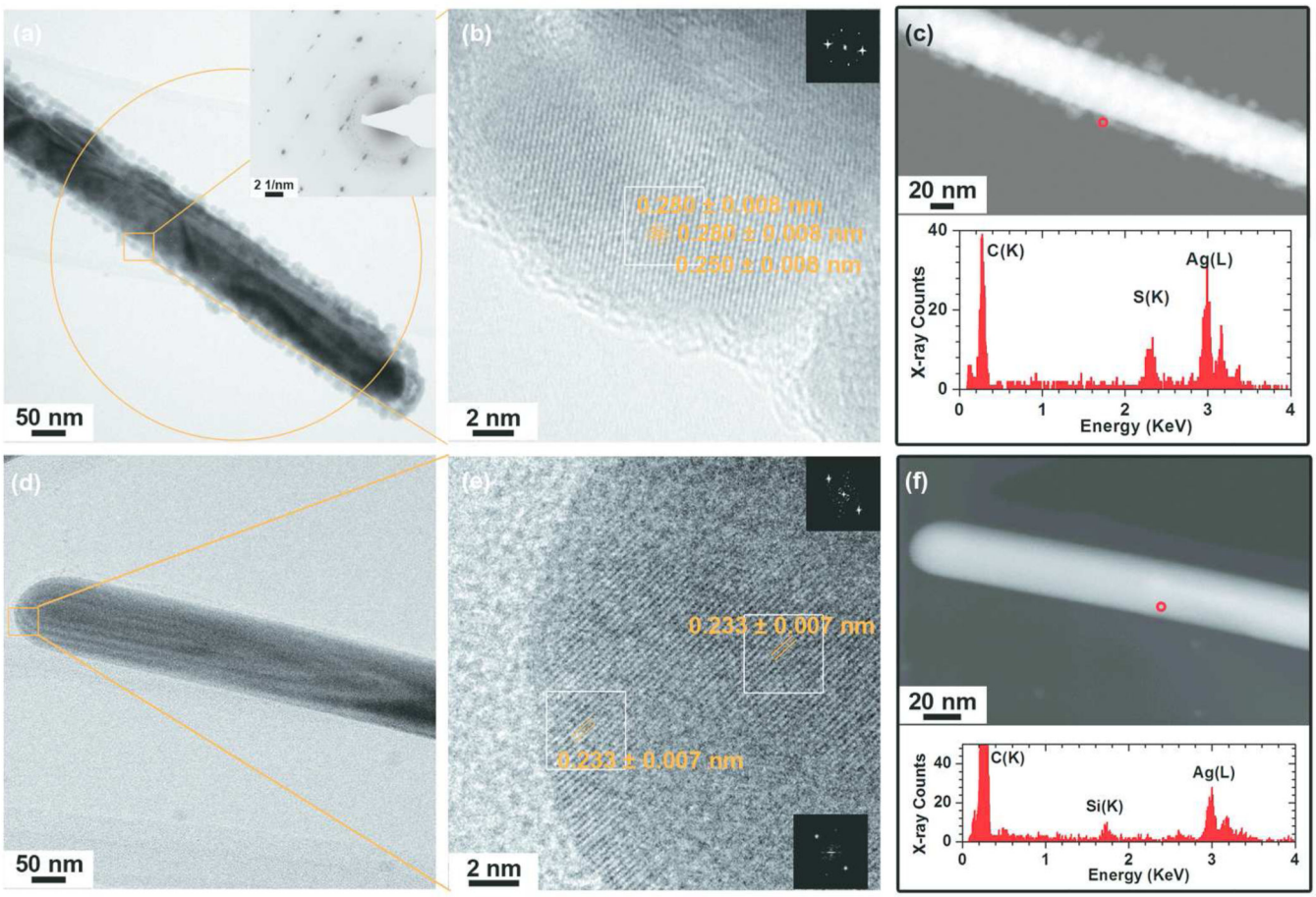

Figure 4.

Physicochemical characterization of AgNWs incubated for 6h at 37 ° C, in: (a–c) small molecule solutes and salts extracted from DCCM-1, (d–f) PBS/proteins extracted from DCCM-1. (a) A representative BF-TEM image of the AgNWs. The inset is a SAED pattern obtained from the circled area (aperture size ~550 nm). (b) HRTEM image taken from the area boxed in Fig. 4a. FFT patterns taken from the boxed areas are inserted. (c-top) HAADF-STEM image obtained from the same area as Fig. 4a. An EDX spectrum collected from the edge of the nanowire (circled in Fig. 4c-top), is shown in (c-bottom). (d) A BF-TEM image of the AgNWs. (e) HRTEM image taken from the boxed area in Fig. 4d. (f) A HAADF-STEM image of the AgNWs (top) and EDX spectrum (bottom) recorded at the surface of the AgNWs (circled in Fig. 4f-top). The silicon peak arises from contamination on the carbon coated TEM grid.[42]

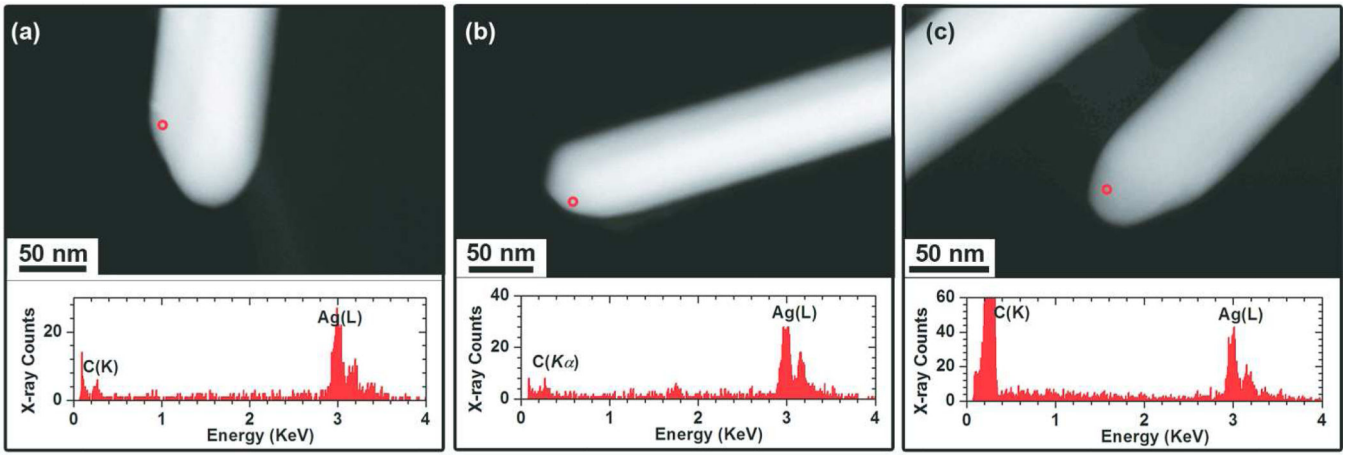

Figure 5.

Physicochemical characterization of AgNWs incubated for 6h at 37 °C, in: (a) PBS, (b) PBS/cysteine and (c) PBS/BSA. HAADF-STEM images of the AgNWs (top) and the corresponding EDX spectra (bottom) collected from the circled regions in the images.

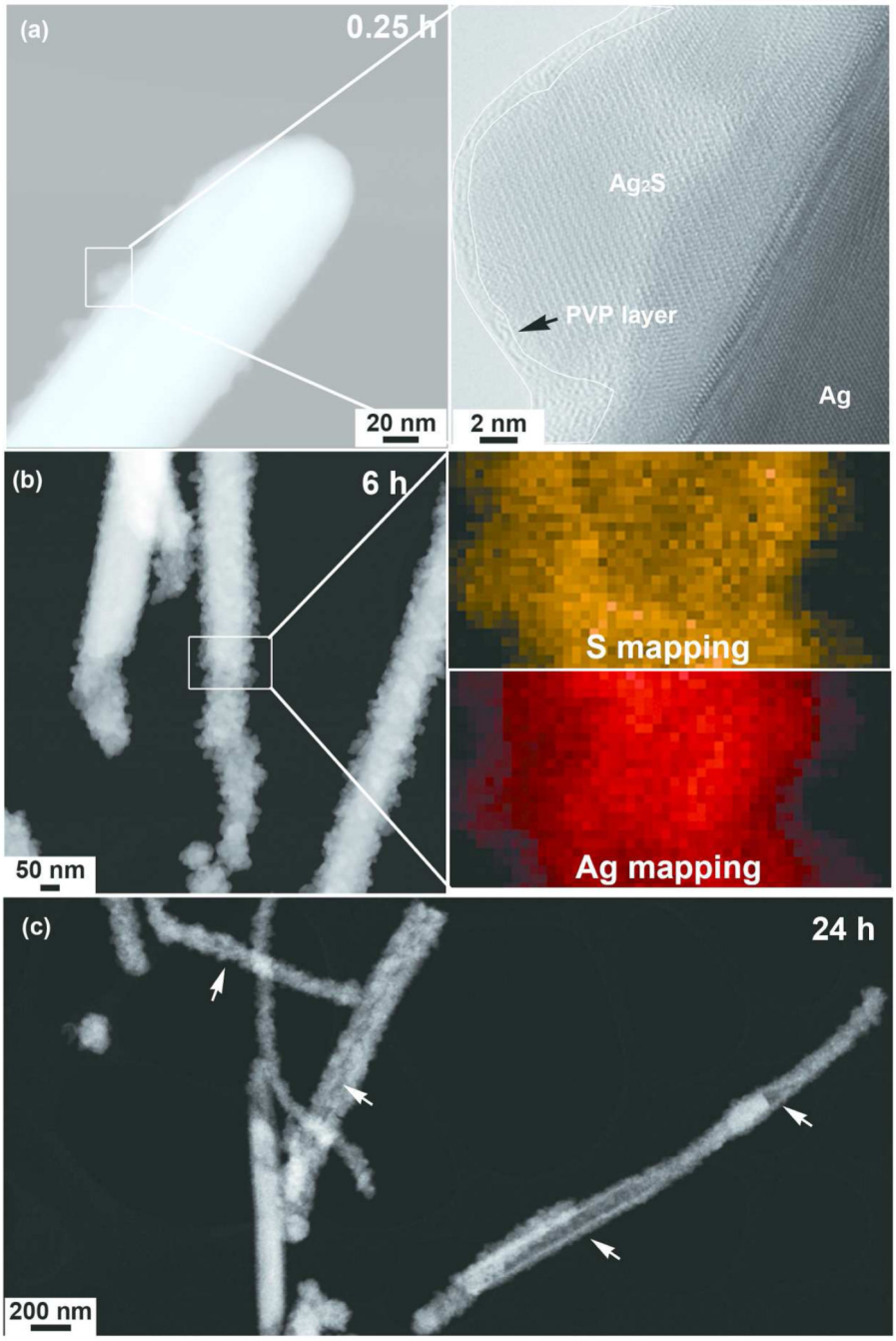

Figure 6.

HAADF-STEM images showing the morphological evolution and sulfidation process of AgNWs incubated in DCCM-1 medium for (a-left) 0.25 h, (b-left) 6 h and (c) 24 h. An HRTEM image (a-right) taken from the boxed area in Fig.6a-left shows the presence of a PVP layer(s) on sulfidized AgNWs surface. The PVP layer which shows a weaker contrast intensity and amorphous morphology is delineated using a white contour. The boxed area in Fig. 6b was further characterized by STEM-EDX Ag and S elemental mapping (Fig. 6b-right). The morphological evolution of the AgNWs in DCCM-1, as a function of time was

characterized by HAADF-STEM. After incubation in DCCM-1 at 37 °C for 0.25 h, a thin surface layer of crystals was present (Fig. 6a-left). A HRTEM image of 24 h sample is presented in SI, Fig 13S.